Brief Communication

MOLECULAR METABOLISM

Loss of hypothalamic Furin affects POMC to proACTH cleavage and feeding behavior in high-fat diet-fed mice

Ilaria Coppola [1], Bas Brouwers [1], Leanne Walker [2], Ceyhun Alar [3], Sandra Meulemans [1], Anne White [2,], Bruno Ramos-Molina [1,4,*], John W.M. Creemers [1,***]**

ABSTRACT

Objective: The hypothalamus regulates feeding and glucose homeostasis through the balanced action of different neuropeptides, which are cleaved and activated by the proprotein convertases PC1/3 and PC2. However, the recent association of polymorphisms in the proprotein convertase *FURIN* with type 2 diabetes, metabolic syndrome, and obesity, prompted us to investigate the role of FURIN in hypothalamic neurons controlling glucose and feeding.

Methods: POMC-Cre$^{+/-}$ mice were bred with *Furin*$^{fl/fl}$ mice to generate conditional knockout mice with *Furin*-deletion in neurons expressing proopiomelanocortin (POMC*Fur*KO), and *Furin*$^{fl/fl}$ mice were used as controls. POMC*Fur*KO and controls were periodically monitored on both normal chow diet and high fat diet (HFD) for body weight and glucose tolerance by established *in-vivo* procedures. Food intake was measured in HFD-fed *Fur*KO and controls. Hypothalamic *Pomc* mRNA was measured by RT-qPCR. ELISAs quantified POMC protein and resulting peptides in the hypothalamic extracts of POMC*Fur*KO mice and controls. The *in-vitro* processing of POMC was studied by biochemical techniques in HEK293T and CHO cell lines lacking FURIN.

Results: In control mice, *Furin* mRNA levels were significantly upregulated on HFD feeding, suggesting an increased demand for FURIN activity in obesogenic conditions. Under these conditions, the POMC*Fur*KO mice were hyperphagic and had increased body weight compared to *Furin*$^{fl/fl}$ mice. Moreover, protein levels of POMC were elevated and ACTH concentrations markedly reduced. Also, the ratio of α-MSH/POMC was decreased in POMC*Fur*KO mice compared to controls. This indicates that POMC processing was significantly reduced in the hypothalami of POMC*Fur*KO mice, highlighting for the first time the involvement of FURIN in the cleavage of POMC. Importantly, we found that *in vitro*, the first stage in processing where POMC is cleaved into proACTH was achieved by FURIN but not by PC1/3 or the other proprotein convertases in cell lines lacking a regulated secretory pathway.

Conclusions: These results suggest that FURIN processes POMC into proACTH before sorting into the regulated secretory pathway, challenging the dogma that PC1/3 and PC2 are the only convertases responsible for POMC cleavage. Furthermore, its deletion affects feeding behaviors under obesogenic conditions.

Keywords FURIN; POMC; proACTH; ACTH; Hypothalamus; Obesity

1. INTRODUCTION

The hypothalamus is a key region of the central nervous system that regulates feeding behavior and energy expenditure in mammals. The melanocortin system is a crucial molecular circuit controlling feeding and metabolism within the arcuate nucleus of the hypothalamus [1]. This circuit includes two antagonistic neuronal populations: the agouti-related protein (AgRP)/neuropeptide Y (NPY) neurons, which stimulate feeding behavior, and the pro-opiomelanocortin (POMC) neurons, which stimulate satiety after a meal [2–4]. Both neural circuits are tightly regulated by peripheral hormones (e.g. leptin and insulin) and neuropeptides through the binding to their neuronal surface receptors [5].

[1]Laboratory for Biochemical Neuroendocrinology, Department of Human Genetics, KU Leuven, Leuven 3000, Belgium [2]Division of Diabetes, Endocrinology & Gastroenterology, School of Medical Sciences, Faculty of Biology, Medicine and Health, University of Manchester, 3.016 AV Hill Building, Manchester M13 9PT, United Kingdom [3]Laboratory of Multi-omic Integrative Bioinformatics, Department of Human Genetics, KU Leuven, Leuven 3000, Belgium [4]Obesity and Metabolism Research Laboratory, Biomedical Research Institute of Murcia (IMIB), Murcia 30120, Spain

*Corresponding author. Obesity and Metabolism Research Laboratory, Biomedical Research Institute of Murcia (IMIB), Murcia, 30120, Spain. E-mail: bruno.ramos@imib.es (B. Ramos-Molina).

***Corresponding author. Laboratory for Biochemical Neuroendocrinology, Department of Human Genetics, KU Leuven, Leuven 3000, Belgium. E-mail: john.creemers@kuleuven.be (J.W.M. Creemers).

**Corresponding author. Division of Diabetes, Endocrinology & Gastroenterology, School of Medical Sciences, Faculty of Biology, Medicine and Health, University of Manchester, 3.016 AV Hill Building, Manchester M13 9PT, United Kingdom. E-mail: anne.white@manchester.ac.uk (A. White).

Received July 8, 2022 • Revision received October 23, 2022 • Accepted October 28, 2022 • Available online 29 October 2022

https://doi.org/10.1016/j.molmet.2022.101627

Abbreviations

α-MSH	α-melanocyte-stimulating hormone
ACTH	adrenocorticotropic hormone
AgRP	agouti-related protein
HEK	human embryonic kidney
HFD	high fat diet
IR	insulin receptor
ISG	immature secretory granule
PC	proprotein convertase
POMC	pro-opiomelanocortin
NCD	normal chow diet
NPY	neuropeptide Y
TGN	*trans*-Golgi network

Endocrine hormones and neuropeptides convey signals between the hypothalamus and other metabolic organs inducing either satiety or appetite. These ligands, as well as many of their cell surface receptors, are synthesized as inactive precursor proteins and require the proteolytic activity of specific endopeptidases as a first step towards activation [6]. After these cleavage steps by endopeptidases, further trimming and amidation are often needed for full activation [7,8]. Most of the cleavages are performed by proprotein convertases (PCs), a seven-member family of subtilisin-like serine proteases with selectivity for basic amino acid motifs [9]. Any alteration of this enzyme—substrate balance can lead to dramatic changes in feeding behaviors and energy metabolism. In particular, both PC1/3 and PC2 are active in the regulated secretory pathway of the neuroendocrine system and are involved in the proteolytic cleavage of hormones and neuropeptides that modulate energy and glucose balance. For instance, cells expressing PC1/3 cleave POMC into adrenocorticotropic hormone (ACTH) and β-lipotropin. Cells expressing PC2, either with or without PC1/3, cleave ACTH further into α-melanocyte-stimulating hormone (α-MSH) [10,11]. An example of the altered enzyme—substrate balance is represented by PC1/3-deficient patients that suffer from early-onset obesity and hyperphagia, together with other endocrinopathies [12,13]. In addition, several polymorphisms and rare heterozygous mutations in the human *PCSK1* gene (encoding for PC1/3) have been associated with an increased risk of obesity [14—16]. So far there are no reported *PCSK2* (encoding for PC2) null patients, but several studies have associated *PCSK2* SNPs with type 2 diabetes risk [17—19]. In this regard, *Pcsk2* knockout mice have chronic mild hypoglycemia and hyperplasia of the pancreatic α-cells [20].

While PC1/3 and PC2 have been extensively studied in the context of obesity and metabolic dysfunction, very little is known about the role of the other PCs in these pathologies. In contrast to PC1/3 and PC2, FURIN, PC5/6, PACE4, and PC7 are mainly active in the constitutive secretory pathway. Within this pathway, FURIN is concentrated in the *trans*-Golgi network (TGN), but it also displays significant enzymatic activity in the endosomes, and at the cell surface. The finding that FURIN is also present in immature secretory granules (ISGs) suggests a possible role for FURIN in the cleavage of substrates present in the regulated secretory pathway [21,22]. For instance, FURIN has been demonstrated to cleave the PC1/3 inhibitor pro-SAAS and the PC2 inhibitor 7B2, but these cleavages are likely taking place early in the secretory pathway before sorting into ISGs [23—25]. Other FURIN substrates involved in energy and glucose homeostasis include the integral subunit of the V-ATPase proton pump, Ac45, and the insulin receptor (IR). In pancreatic beta cells, FURIN has been shown to be essential for the proteolytic activation of Ac45, affecting granule and lysosomal acidification [26,27]. Also in beta cells, FURIN activity is involved in IR activation, and therefore in the regulation of insulin signaling [28]. In addition, the IR is a FURIN substrate in several cancer cell lines and specific mouse tissues [28—30]. Importantly, IR has a crucial role in the central nervous system in controlling systemic glucose balance [31—33]. However, the precise mechanism by which FURIN regulates energy and glucose homeostasis is still undefined and might involve other substrates as well.

In this study, we have investigated the role of FURIN in POMC processing and maturation, and we have determined the role of hypothalamic FURIN *in vivo* by deleting *Furin* in POMC neurons.

2. MATERIALS AND METHODS

2.1. Cell culture and transfection

The human embryonic kidney (HEK) 293 T cell line was cultured in DMEM/F-12 without phenol red (Thermo Fisher Scientific) supplemented with 10% heat-inactivated fetal bovine serum, 100 U/ml penicillin, and 100 μg/ml streptomycin. 24 h after seeding, cells (≈60% confluency) were transfected with plasmids encoding human c-myc-tagged-*POMC* plasmid (within pcDNA3 backbone) and human *FURIN*, or *PCSK1*, mouse *Pcsk5A*, *Pcsk5B*, *Pcsk6* or human *PCSK7* using X-tremeGENE™ 9 (Roche) according to the manufacturer's protocol. As negative control, cells were transfected with pcDNA3 plasmid, indicated in Figure 4A—B and Figure 1 as mock.

2.2. Western blot

Cells were lysed in 1× lysis buffer (20 mM Tris—HCl (pH 7.5), 150 mM NaCl, 1 mM Na_2EDTA, 1 mM EGTA, 1% Triton, 2.5 mM sodium pyrophosphate, 1 mM beta-glycerophosphate, 1 mM Na_3VO_4, 1 μg/ml leupeptin (Cell Signaling Technology)). The conditioned media were collected for methanol precipitation after overnight incubation of the cells in 1 mL of serum free medium (DMEM/F-12 without phenol red). 12.5 μg of BSA were added as control of methanol precipitation. The precipitated proteins were dissolved in 1× sample buffer (Tris base 0.0625 M, SDS 0.07 M (2%), glycerol 10%, bromophenol blue) and prepared for western blot. Western blot was performed according to the standard procedures using NuPAGE 10% Bis-Tris minigels and NuPAGE MES SDS running buffer 1× (Thermo Fisher Scientific). The primary antibodies used were mouse anti-myc (homemade), and anti-ACTH (clone A2A3, RRID: 2905636) directed against the C-terminus of ACTH so can recognize proACTH. Mouse anti-FURIN (MON152 [34]), and rabbit anti-PC1/3, anti-PC5/6 A, anti-PC5/6 B, anti-PACE4, and anti-PC7 (homemade) were used to detect each PC in either cell lysates or conditioned media. The secondary antibodies were anti-mouse or anti-rabbit labeled with horseradish peroxidase (HRP) (Dako).

2.3. Generation of POMC*Fur*KO mice

POMC-Cre$^{+/-}$ (B6·FVB-Tg (Pomc-cre) 1Lowl/J, JAX stock #010714) mice were bought from Jackson Laboratories (https://www.jax.org). *Furin*$^{fl/fl}$ mice were described before [35]. Mice were backcrossed at least 5 times to a C57Bl6J background. All the mice were housed in standard cages on a 12-hour day/night cycle and fed a standard rodent chow (10 KJ% fat, 13 KJ% protein, 77 KJ% carbohydrates) or high fat diet (HFD) (45 KJ% fat (Lard), 20 KJ% protein, 35 KJ% carbohydrates) in a conventional facility of the KU Leuven. Food and water were provided *ad libitum*. All experiments were approved by the KU Leuven Animal Welfare Committee, following the guidelines provided in the Declaration of Helsinki (KU Leuven project number 034/2020). For food intake experiments, POMC-Cre mice were individually housed in single grid cages with 5 days of acclimatization and 3 days of food intake measurements.

2.4. Intraperitoneal glucose tolerance test (IPGTT)

Mice were fasted overnight or 4 h and intraperitoneally injected with 1.5–2 mg/g body weight of D-glucose in PBS. Blood glucose levels were monitored at indicated time-points using a Contour Glucometer (Roche).

2.5. Real time quantitative PCR (RT-qPCR)

RNA from snap frozen mouse hypothalamus was isolated using the Nucleospin RNA II (Macherey Nagel) kit according to the manufacturer's protocol. cDNA was synthetized using the iScript cDNA synthesis kit (Bio-Rad). Primers were designed using the Primer 3 plus software. RT-qPCR was performed with a CFX Connect Real-Time PCR Detection System from Bio-Rad using SYBR Green supermix (Bio-Rad). Data is represented as $2^{-\Delta\Delta Ct}$. Primers for mouse genes and the *Cre* recombinase gene from bacteriophage P1 are listed in Table S1.

2.6. Peptide isolation from hypothalamus

Hypothalamic extracts were generated based on the technique in [36]. Extractions were optimized for each protein/peptide using known amounts of the protein/peptide spiked into the hypothalamus and recovery/interference assessed. Each frozen hypothalamus was disrupted in cold 0.1 M HCl using a Qiagen TissueRuptor. The resulting homogenates were centrifuged at 5000 g at 4 °C for 20 min and supernatants transferred to a low-protein retention tube. A 50 μL aliquot was removed to a separate tube for total protein measurement using a BCA protein assay (see below), then a stabilizing buffer of 0.1 M tris/0.1% BSA was added to the extracts before freezing at −80 °C. The hypothalamic extracts were diluted 1:3 with 1× PBS/1% BSA for measurement in the POMC, ACTH, and α-MSH ELISAs.

2.7. POMC ELISA

The total POMC in each hypothalamus was detected by using a 2-site immunometric assay with monoclonal antibodies, as described previously [11,37,38]. Briefly, monoclonal antibody A1A12 (RRID: 2756529) which binds the central ACTH region 10–18, was coated on the ELISA plate. After the addition of standards or samples, a biotin-labelled N1C11 monoclonal antibody (specific for the gamma MSH region of POMC; RRID: 2756530) was added, followed by HRP-labeled avidin as well as the enzyme substrate for the final detection. This assay has a sensitivity of 10 pmol/L and is specific for POMC and proACTH, and does not detect ACTH or α-MSH [39].

2.8. ACTH ELISA

The ACTH detection and quantification in mouse hypothalamic samples was performed by using a 2-site immunometric assay as described [11,37]. Briefly, The ACTH ELISA plates were coated with monoclonal antibody A1A12 (RRID: 2756529). The detection antibody was monoclonal antibody A2A3 (RRID: 2905636), directed against the C-terminus of ACTH, and labeled directly with HRP. The standards were prepared from human pituitary ACTH, provided by the National Institute of Biological Standards and Control, London, UK. This assay has a sensitivity of 1.1 pmol/L and has previously been shown to have <0.1% cross reactivity with POMC and does not detect α-MSH, ACTH 18–39 or ACTH 1–24.

2.9. α-MSH ELISA

Detection and quantification of α-MSH was performed by using a newly developed competitive ELISA based on a single polyclonal antibody (RRID: 2756515) produced by Prof. Sharon Wardlaw, Columbia University [40,41]. This antibody is specific for C-terminal amidated α-MSH, and shows no cross reactivity with POMC, ACTH, or the free acid form of α-MSH that has not been amidated. The antibody (1 mg/L) was added to an ELISA plate previously coated with 10 mg/L rabbit anti-IgG (Sigma Aldrich, UK). Biotin labelled α-MSH (created by combining biotin and α-MSH at a 50:1 M ratio) was added to the wells at 100 pmol/L, followed by α-MSH standards (Abcam) in the range of 15–1000 pmol/L) or samples. The unlabeled standards or samples competed with the labelled α-MSH to bind the polyclonal anti-α-MSH

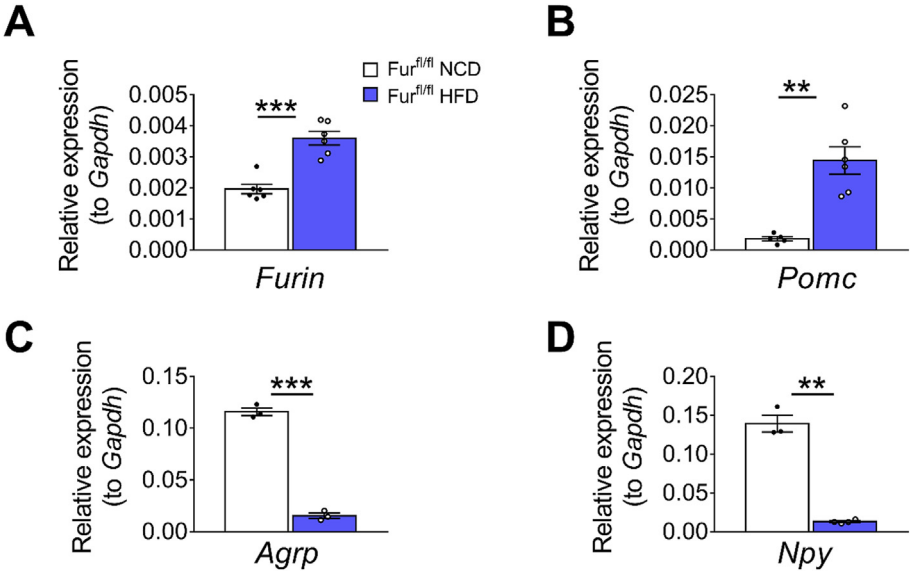

Figure 1: Furin and Pomc mRNA levels are increased by a chronic high-fat-diet in Fur$^{fl/fl}$ control mice. Relative mRNA expression in hypothalami of 23-week-old male Fur$^{fl/fl}$ mice fed either a NCD or a HFD for 15 weeks. The mice were in a fed state at the moment of the euthanasia (A) Furin, (B) Pomc, (C) Agrp, (D) Npy. n = 3–6 mice/group. **P < 0.01, ***P < 0.001, determined by unpaired t test with Welch's correction. All the values were normalized to Gapdh expression and data are represented as mean ± SEM. NCD: normal chow diet; HFD: high fat diet.

antibody. Then, avidin-labelled HRP and the enzyme substrate were added to generate the signal measured at OD 450 nm. This assay has a sensitivity of 20 pmol/L.

2.10. Bicinchoninic acid (BCA) protein assay

Hypothalamus extracts were diluted 1:9 with 1× PBS and total protein quantified using the Pierce RapidGold BCA protein assay kit (Thermofisher Scientific). The assay was performed according to the manufacturers' instructions.

2.11. Metabolic labeling experiment

Transfected cells were metabolically labelled as described before [42]. After 40 min pulse labelling with 1 mCi ^{35}S-methionine the cells were lysed and the lysates immune-precipitated with A2A3 and myc antibodies bound to protein G sepharose (Pharmacia Biotech).

2.12. Statistical analysis

Results are expressed as means ± SEM. Statistical analysis was performed by unpaired Student's t test or one-way ANOVA with Sidak's multiple comparisons test for grouped analysis, or repeated measure two-way ANOVA for pairwise time-specific differences between genotypes. A value of $p < 0.05$ was considered significant. $^{*}p < 0.05$, $^{**}p < 0.01$, $^{***}p < 0.001$.

3. RESULTS

We found that hypothalamic *Furin* mRNA levels were increased twofold in the group of control (*Fur*$^{fl/fl}$) mice on HFD compared to control animals on a normal chow diet (NCD), suggesting that FURIN activity might be important in regulating energy homeostasis (Figure 1A). *Pomc* expression was also strongly increased (Figure 1B), while *Agrp*

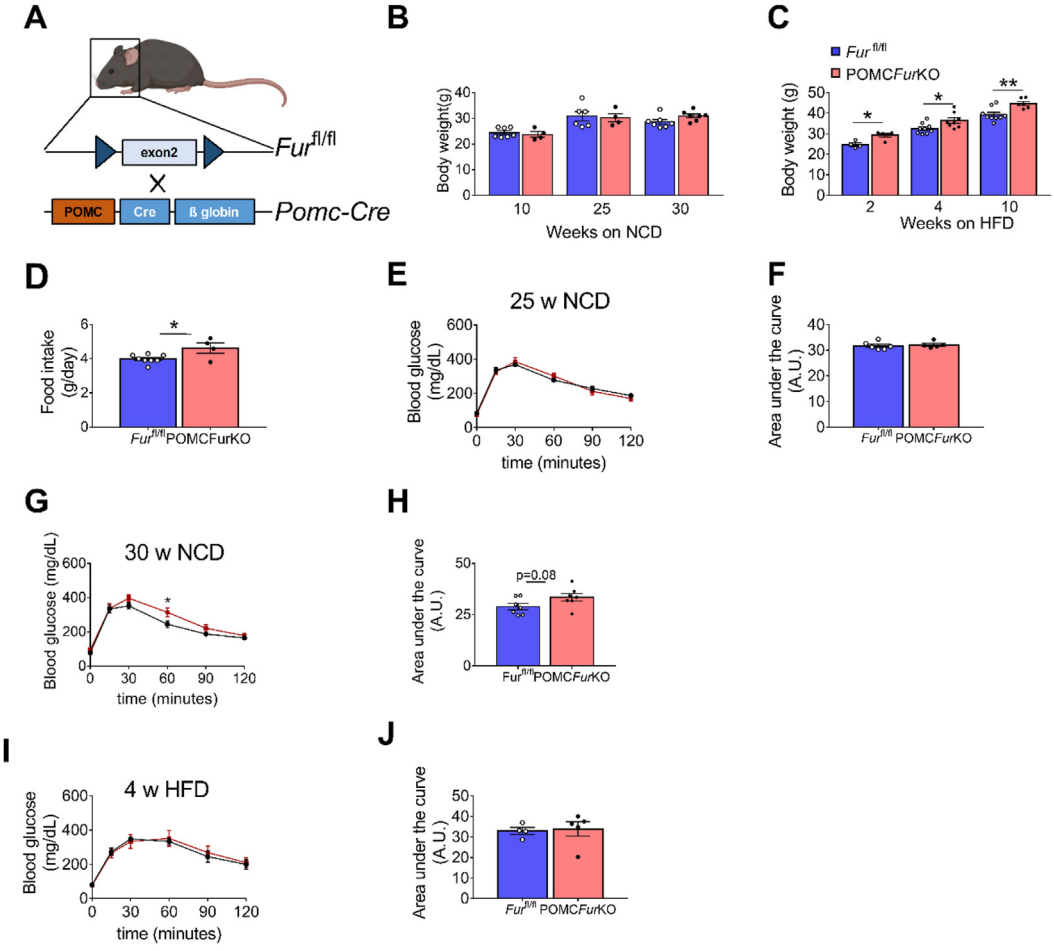

Figure 2: The absence of Furin in POMC-neurons leads to hyperphagia and increased body weight after a short HFD period. (A) Schematic of the breeding strategy used to generate the POMCFurKO mice. Female mice with the exon 2 of the Furin gene flanked by two loxP sites (Fur$^{fl/fl}$) were bred with male mice expressing the Cre recombinase under the control of the POMC promoter (POMC-Cre). Fur$^{fl/fl}$ are used as controls; POMC-Cre$^{+/-}$, Fur$^{fl/fl}$ mice are referred to as POMCFurKO. (B) Body weight of random NCD-fed male POMCFurKO and Fur$^{fl/fl}$ mice of 10, 25, 30 weeks of age (n = 5–9 mice/group). No significant differences were observed by one-way ANOVA with Sidak's multiple comparisons test. (C) Body weight of 10, 12, and 18-week-old mice after 2, 4, and 10 weeks of HFD respectively (n = 4–9 mice/group). $^{*}P < 0.01$; $^{*}P < 0.05$ determined by one-way ANOVA with Sidak's multiple comparisons test. (D) Daily food intake (g) of 11-week-old male POMCFurKO and Fur$^{fl/fl}$ mice on HFD for 3 weeks. Data are represented as the average over three days (n = 4–8 mice/group). $^{*}P < 0.05$ determined by unpaired t-test. (E) IPGTT on 25-week-old POMCFurKO and Fur$^{fl/fl}$ male mice on NCD after overnight fasting (n = 5–6 mice/group). (F) The area under the curve in E was expressed as g/dL/120 min. (G) IPGTT on 30-week-old POMCFurKO and Fur$^{fl/fl}$ male mice on NCD after overnight fasting (n = 7 mice/group). $^{*}P < 0.05$ determined by two-way ANOVA with Sidak's multiple comparisons test. (G) The area under the curve in G was expressed as g/dL/120 min. (G) IPGTT on 12-week-old POMCFurKO and Fur$^{fl/fl}$ male mice on HFD for 4 weeks after overnight fasting (n = 3 mice/group). (H) The area under the curve in G was expressed as g/dL/120 min. No significant differences were observed by unpaired t-test. NCD: normal chow diet; HFD: high fat diet.

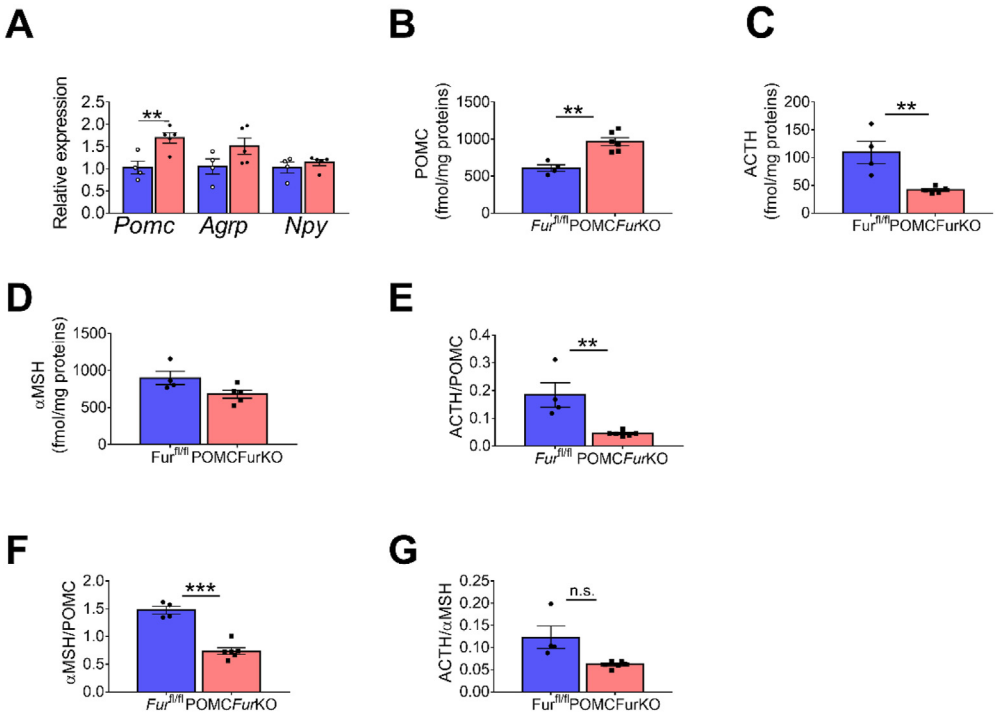

Figure 3: POMC expression and processing is altered in HFD-fed POMCFurKO mice. (A) Relative mRNA expression of Npy, Agrp, and Pomc in the hypothalami of 10-week-old male POMCFurKO (pink bars) and $Fur^{fl/fl}$ (blue bars) mice on HFD for 2 weeks (n = 4–5 mice/group). **P < 0.01 determined by unpaired t-test. All data are represented as mean ± SEM. The total content of POMC (B), ACTH (C), αMSH (D), and the ratio ACTH/POMC (E), αMSH/POMC (F), and ACTH/αMSH (G) in the hypothalami of 11-week-old male POMCFurKO and $Fur^{fl/fl}$ mice fed on HFD for 3 weeks (n = 4–6 mice/group). **P < 0.01; ***P < 0.001 determined by unpaired t-test. For RT-qPCR analyses, the values were normalized to Gapdh expression levels; all data are represented as mean ± SEM. (For interpretation of the references to color in this figure legend, the reader is referred to the Web version of this article.)

and *Npy* were decreased (Figure 1C–D), consistent with previous studies with HFD-diet fed mice [43–45].

To establish the possible role of hypothalamic FURIN in controlling energy and glucose homeostasis, we generated a conditional knockout mouse model in which *Furin* was deleted in POMC neurons. *Pomc-Cre*$^{+/-}$ mice were bred with $Fur^{fl/fl}$ mice to study the potential role of *Furin* specifically in anorexigenic POMC neurons (Figure 2A). We confirmed the Cre-mediated *Furin* recombination by RT-qPCR analysis of both *Furin* (lacking exon 2) and *Cre* mRNA in the hypothalamus of POMC*Fur*KO and $Fur^{fl/fl}$ mice (Fig. S1). When fed on NCD, body weight of POMC*Fur*KO mice was similar to $Fur^{fl/fl}$ control mice (Figure 2B). However, on HFD POMC*Fur*KO mice became significantly heavier than $Fur^{fl/fl}$ mice from 2 weeks of HFD onwards (Figure 2C). Consistent with the increase in body weight, food intake of POMC*Fur*KO mice was significantly higher than $Fur^{fl/fl}$ mice after 3 weeks of HFD (Figure 2D). A subset of glucose sensing POMC neurons regulate glucose homeostasis, and are defective in obesity [46]. To investigate if the loss of FURIN negatively affects these neurons, we performed glucose tolerance tests on POMC*Fur*KO and control mice on both normal and high-fat regimens (Figure 2E–J and S2). Glucose tolerance was normal in POMC*Fur*KO and $Fur^{fl/fl}$ mice on NCD (Figure 2E–F and S2A-B), with a mild glucose intolerance only observed in 30-week-old POMC*Fur*KO mice (Figure 2G–H). A HFD challenge did not alter glucose tolerance in POMC*Fur*KO mice compared to controls (Figure 2I–J and S2C–F). Normal fasting blood glucose levels were observed in POMC*Fur*KO mice, either on NCD at 10, 25, and 30 weeks of age or after 4 and 10 weeks of HFD (Fig. S2G–H). These results suggest that the absence of FURIN in POMC neurons did not significantly affect glucose homeostasis despite the clear impact on body weight and appetite.

Pomc expression levels in POMC*Fur*KO mice were significantly higher than in the controls, while the mRNA expression levels of *AgRP* and *Npy* were not changed (Figure 3A). At protein level, the absolute amount of POMC was increased in hypothalamic lysates of HFD-fed POMC*Fur*KO mice (Figure 3B), whereas ACTH was significantly decreased (Figure 3C), and α-MSH slightly reduced, although not significantly (Figure 3D). The ACTH and α-MSH amounts relative to POMC were strongly decreased, indicating defective POMC processing (Figure 3E–F). The ACTH relative to the α-MSH content was decreased, albeit not significantly (Figure 3G).

In order to determine whether POMC processing was directly dependent on FURIN activity, we analyzed the *in-vitro* processing of the POMC precursor in Δ*Fur*HEK293T cells, lacking FURIN, co-transfected with *POMC* and FURIN, PC1/3, PACE4, PC5/6 A, PC5/6 B, or PC7. (Figure 4). PC4 was not included because it is germ-cell specific and PC2 because it is not active in cells without a regulated secretory pathway. The POMC detected in the cell lysates of Δ*Fur*-HEK293T cells was equally present and each PC was efficiently expressed in each experimental condition (Figure 4A–B). The resulting POMC cleavage products were detected in the conditioned media and in the cell lysate of Δ*Fur*HEK293T cells (Figure 4C–D). Interestingly, FURIN was the only PC able to efficiently cleave POMC at the cleavage site KR164↓ resulting mainly in 23 KDa proACTH. A minute amount of glycosylated and mature ACTH forms (gACTH and mACTH, respectively) could be detected after prolonged exposure. PC7 was able to cleave the same consensus site, albeit much less efficiently (Figure 4C). Under these conditions, in the absence of a regulated secretory pathway, PC1/3 was unable to cleave POMC. These results are consistent with previous studies showing that

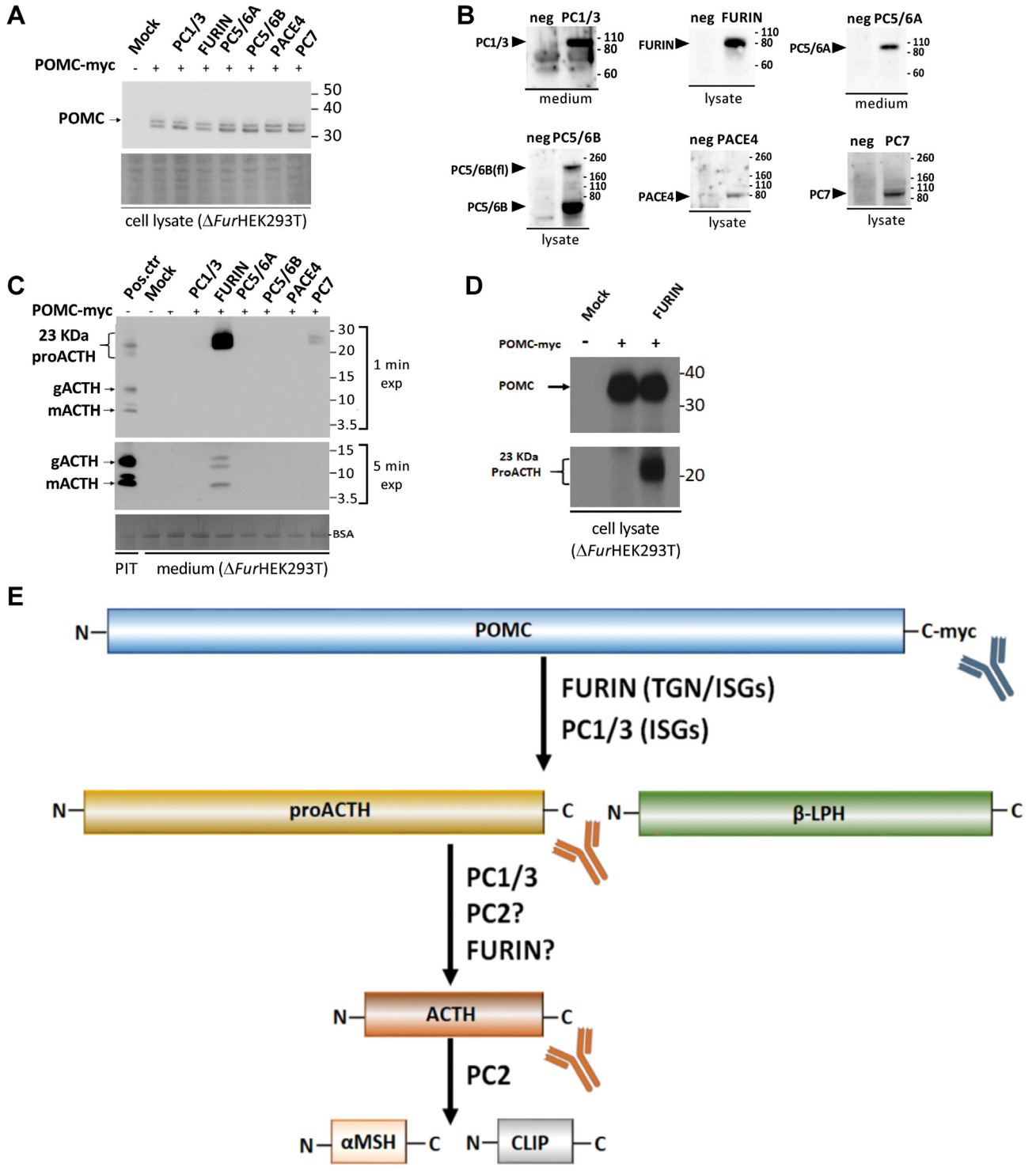

Figure 4: POMC is selectively cleaved by FURIN at the C-terminal site of ACTH (KR164↓) into proACTH and β-lipotropin (LPH) in ΔFurHEK293T cells. Western blot analysis of POMC and each co-transfected PCs in cell lysate (A—B) and proACTH and ACTH in medium (C) of Furin-deficient HEK293T cells co-transfected with POMC and different PCs. The blot in A (upper panel) is labeled with an anti-myc antibody. The lower panel shows a ponceau S-staining of the cell lysates as loading reference. (B) Western blot analysis of each transfected PC detected either in the medium or in the cell lysate. As negative control was used medium or cell lysate from ΔFurHEK293T transfected with a different PC. The blot in C is labeled with the A2A3 antibody directed against the free carboxy-terminus of ACTH. One minute-exposure of the entire blot (upper panel), and 5 min-exposure of the lower part of the blot (lower panel) to show the less abundant low MW ACTH forms. Mouse pituitary protein extract (25 μg) was used as positive control (first lane). (D) Metabolic labeling of Furin-deficient HEK293T cells transfected with POMC alone or together with FURIN (40 min pulse). (E) New model for POMC processing in hypothalamus. The antibody used to detect POMC-myc is depicted in blue, and in orange the antibody used to detect proACTH and ACTH (glycosylated: gACTH, and mature: mACTH). In ΔFurHEK293T cells lacking the secretory pathway, FURIN preferentially cleaves the first POMC cleavage site, most likely in the TGN. The same cleavages are mediated by PC1/3 in cells with a regulated secretory pathway probably requiring the pH conditions of the ISGs. Cleavage of proACTH to ACTH is performed by PC1/3, the enzymes providing redundancy are probably FURIN and/or PC2. (For interpretation of the references to color in this figure legend, the reader is referred to the Web version of this article.)

prorenin cannot be cleaved by PC1/3 in cells lacking a regulated secretory pathway but is cleaved in neuroendocrine cells [47,48]. It was suggested that the carboxyterminal tail of PC1/3, which is cleaved off in secretory granules, has an autoinhibitory function in the TGN. Moreover, POMC was cleaved to proACTH by FURIN inside the Δ*Fur*HEK293T cells after a short 40 min pulse labeling, which allows newly synthesized protein to reach the TGN, but is too short for secretion (Figure 4D). A schematic of POMC cleavage mediated by FURIN, together with the specific antibodies used to detect POMC, proACTH and ACTH, is represented in Figure 4E. To corroborate these unexpected results that challenge the dogma that only PC1/3 and PC2 are involved in the processing of POMC into ACTH/α-MSH, we repeated these experiments in FURIN deficient CHO cells (RPE.40 cells [49]) with similar results (Fig. S3).

4. DISCUSSION

In this study, we have demonstrated that hypothalamic *Furin* in mice is essential for the regulation of energy homeostasis under obesogenic conditions. Our results revealed that the absence of *Furin* in POMC neurons caused an increase in body weight and food intake on HFD. In addition, we demonstrated that FURIN-dependent processing of neuropeptides in feeding-controlling neurons can be linked to the metabolic state of the animals. This is consistent with the 2-fold increased expression of *Furin* during HFD compared to the NCD in control mice. Most remarkable is our observation that FURIN is most likely a POMC to proACTH convertase in the hypothalamus.

The hyperphagia and increased body weight observed in POMC*Fur*KO mice suggest the melanocortin system as a potential source of FURIN substrates linked to the phenotype. PC1/3 and PC2 have generally been considered the only PC processing enzymes of POMC [8]. Our *in vitro* findings put FURIN forward as a new enzymatic player of the melanocortin system involved in the first cleavage step of POMC that normally takes place in the TGN/immature granules [50,51]. These results are further corroborated by both the increased amount of the POMC protein as well as the mRNA level in POMC*Fur*KO hypothalami and the hyperphagia during obesogenic conditions. Remarkably, mice lacking PC1/3 in adult POMC-expressing neurons do not become obese, neither on NCD nor on a HFD and have a normal amount of ACTH and α-MSH [11], suggesting that POMC can be redundantly cleaved by other PCs, most likely FURIN and PC2, in hypothalamic neurons. The cleavage step of ACTH into α-MSH is exclusively performed by PC2 and PC2 null mice therefore have undetectable levels of α-MSH in hypothalamus [10].

Our results provide evidence for the model presented in Figure 4D. Furin appears to be the only PC able to cleave POMC in the TGN, while PC1/3 can cleave it in ISGs. The subsequent PC cleavage at the aminoterminus of proACTH necessary to generate ACTH can be performed by PC1/3 but possibly also by FURIN based on the near-normal levels of ACTH in PCSK1 null patients [13]. This newly identified role of FURIN in the processing of POMC warrants reassessment of other cleavages of peptide hormones and neuropeptides. For instance, PCSK1 null patients have reduced but detectable amounts of GLP-1 in serum [13,52].

Besides the direct effect that the impaired processing of POMC might have on the phenotype of POMC *Fur*KO mice, loss of FURIN might also affect other substrates which might indirectly affect the melanocortin pathway and therefore the observed phenotype. These substrates include for instance the V-ATPase subunit ATP6AP1/Ac45, shown to be cleaved by FURIN in β cells [26,27], and involved in the acidification and hence secretion of granules [53–55]. However, the activity of PC2, which has an acidic pH optimum, is not severely affected based on the (near) normal amounts of α-MSH.

Furthermore, other molecules, such as semaphorins, crucial for development of the melanocortin system in hypothalamic neurons [56,57] and brain-derived neurotrophic factor (BDNF), which has a crucial role in regulating energy homeostasis [58,59], are potential FURIN substrates and therefore might be possible contributors to the obese-like phenotype.

In conclusion, in this work we have unveiled the importance of FURIN activity in the regulation of energy balance in hypothalamic neurons during a high metabolic challenge. In particular, our results strongly indicate that FURIN activity becomes critical in POMC neurons during a HFD regimen, likely through the proteolytic cleavage of POMC which is required to overcome the augmented metabolic demand.

DATA AVAILABILITY

No data was used for the research described in the article.

ACKNOWLEDGEMENTS

We would like to thank to Prof. Sharon Wardlaw (Columbia University, US) for kindly providing the α-MSH antibody.

This research was funded by FWO Vlaanderen, grant number G0B0617N. B.R.-M. was supported by the "Miguel Servet Type I" program (CP19/00098, ISCIII, Spain; co-funded by the Fondo Europeo de Desarrollo Regional-FEDER). I.C. and B.B. were supported by PhD fellowships (Fundamental Research) from FWO Vlaanderen. The A.W. lab was supported by the Fitzgerald and Mawer endowment funds.

CONFLICT OF INTEREST

None declared.

APPENDIX A. SUPPLEMENTARY DATA

Supplementary data to this article can be found online at https://doi.org/10.1016/j.molmet.2022.101627.

REFERENCES

[1] Myers, M.G., Olson, D.P., 2012 15. Central nervous system control of metabolism. Nature 491(7424):357–363.

[2] Aponte, Y., Atasoy, D., Sternson, S.M., 2011. AGRP neurons are sufficient to orchestrate feeding behavior rapidly and without training. Nature Neuroscience 14(3):351–355.

[3] Zhang, L., Hernandez-Sanchez, D., Herzog, H., 2019. Regulation of feeding-related behaviors by arcuate neuropeptide Y neurons. Endocrinology 160(6): 1411–1420.

[4] Cowley, M.A., Smart, J.L., Rubinstein, M., Cerdán, M.G., Diano, S., Horvath, T.L., et al., 2001. Leptin activates anorexigenic POMC neurons through a neural network in the arcuate nucleus. Nature 411(6836):480–484.

[5] Timper, K., Brüning, J.C., 2017. Hypothalamic circuits regulating appetite and energy homeostasis: pathways to obesity. Disease Models & Mechanisms 10(6):679–689.

[6] Seidah, N.G., Chrétien, M., 1999. Proprotein and prohormone convertases: a family of subtilases generating diverse bioactive polypeptides. Brain Research 848(1–2):45–62.

[7] Lindberg, I., Fricker, L.D., 2021. Obesity, POMC, and POMC-processing enzymes: surprising results from animal models. Endocrinology 162(12): bqab155.

[8] Harno, E., Gali Ramamoorthy, T., Coll, A.P., White, A., 2018. POMC: the physiological power of hormone processing. Physiological Reviews 98(4): 2381–2430.

[9] Creemers, J.W.M., Khatib, A.M., 2008. Knock-out mouse models of proprotein convertases: unique functions or redundancy? Frontiers in Bioscience 13: 4960–4971.

[10] Zhu, X., Zhou, A., Dey, A., Norrbom, C., Carroll, R., Zhang, C., et al., 2002. Disruption of PC1/3 expression in mice causes dwarfism and multiple neuroendocrine peptide processing defects. Proceedings of the National Academy of Sciences of the United States of America 99(16):10293–10298.

[11] Shakya, M., Gahlot, S., White, A., Verchere, C.B., Low, M.J., Lindberg, I., 2021. Mice lacking PC1/3 expression in POMC-expressing cells do not develop obesity. Endocrinology 162:1–15 bqab055.

[12] Aerts, L., Terry, N.A., Sainath, N.N., Torres, C., Martín, M.G., Ramos-Molina, B., et al., 2021. Novel homozygous inactivating mutation in the PCSK1 gene in an infant with congenital malabsorptive diarrhea. Genes 12(5):710.

[13] Jackson, R.S., Creemers, J.W., Ohagi, S., Raffin-Sanson, M.L., Sanders, L., Montague, C.T., et al., 1997. Obesity and impaired prohormone processing associated with mutations in the human prohormone convertase 1 gene. Nature Genetics 16(3):303–306.

[14] Ramos-Molina, B., Martin, M.G., Lindberg, I., 2016. PCSK1 variants and human obesity. Progress in Molecular Biology and Translational Science 140:47–74.

[15] Benzinou, M., Creemers, J.W.M., Choquet, H., Lobbens, S., Dina, C., Durand, E., et al., 2008. Common nonsynonymous variants in PCSK1 confer risk of obesity. Nature Genetics 40(8):943–945.

[16] Creemers, J.W.M., Choquet, H., Stijnen, P., Vatin, V., Pigeyre, M., Beckers, S., et al., 2012. Heterozygous mutations causing partial prohormone convertase 1 deficiency contribute to human obesity. Diabetes 61(2):383–390.

[17] Yoshida, H., Ohagi, S., Sanke, T., Furuta, H., Furuta, M., Nanjo, K., 1995. Association of the prohormone convertase 2 gene (PCSK2) on chromosome 20 with NIDDM in Japanese subjects. Diabetes 44(4):389–393.

[18] Zheng, X., Ren, W., Zhang, S., Liu, J., Li, S., Li, J., et al., 2012 Jan. Association of type 2 diabetes susceptibility genes (TCF7L2, SLC30A8, PCSK1 and PCSK2) and proinsulin conversion in a Chinese population. Molecular Biology Reports 39(1):17–23.

[19] Winters, A., Ramos-Molina, B., Jarvela, T.S., Yerges-Armstrong, L., Pollin, T.I., Lindberg, I., 2017. Functional analysis of PCSK2 coding variants: a founder effect in the Old Order Amish population. Diabetes Research and Clinical Practice 131:82–90.

[20] Furuta, M., Yano, H., Zhou, A., Rouillé, Y., Holst, J.J., Carroll, R., et al., 1997. Defective prohormone processing and altered pancreatic islet morphology in mice lacking active SPC2. Proceedings of the National Academy of Sciences of the United States of America 94(13):6646–6651.

[21] Dittie, A.S., Klumperman, J., Tooze, S.A., 1999. Differential distribution of mannose-6-phosphate receptors and furin in immature secretory granules. Journal of Cell Science 112(22):3955–3966.

[22] Dittié, A.S., Thomas, L., Thomas, G., Tooze, S.A., 1997. Interaction of furin in immature secretory granules from neuroendocrine cells with the AP-1 adaptor complex is modulated by casein kinase II phosphorylation. The EMBO Journal 16(16):4859–4870.

[23] Sayah, M., Fortenberry, Y., Cameron, A., Lindberg, I., 2001. Tissue distribution and processing of proSAAS by proprotein convertases. Journal of Neurochemistry 76(6):1833–1841.

[24] Mzhavia, N., Qian, Y., Feng, Y., Che, F.Y., Devi, L.A., Fricker, L.D., 2002. Processing of proSAAS in neuroendocrine cell lines. Biochemical Journal 361(Pt 1):67–76.

[25] Hwang, J.R., Lindberg, I., 2001. Inactivation of the 7B2 inhibitory CT peptide depends on a functional furin cleavage site. Journal of Neurochemistry 79(2): 437–444.

[26] Louagie, E., Taylor, N.A., Flamez, D., Roebroek, A.J.M., Bright, N.A., Meulemans, S., et al., 2008. Role of furin in granular acidification in the endocrine pancreas: identification of the V-ATPase subunit Ac45 as a candidate substrate. Proceedings of the National Academy of Sciences of the United States of America 105(34):12319–12324.

[27] Brouwers, B., Coppola, I., Vints, K., Dislich, B., Jouvet, N., Lommel, L.V., et al., 2020. Loss of furin in β cells induces an mTORC1-ATF4 anabolic pathway that leads to β cell dysfunction [Internet] Diabetes 70:492–503 [cited 2021 Jan 20]; Available from: https://diabetes.diabetesjournals.org/content/early/2020/11/27/db20-0474.

[28] Coppola, I., Brouwers, B., Meulemans, S., Ramos-Molina, B., Creemers, J.W.M., 2021. Differential effects of furin deficiency on insulin receptor processing and glucose control in liver and pancreatic β cells of mice. International Journal of Molecular Sciences 22(12):6344.

[29] He, Z., Thorrez, L., Siegfried, G., Meulemans, S., Evrard, S., Tejpar, S., et al., 2020. The proprotein convertase furin is a pro-oncogenic driver in KRAS and BRAF driven colorectal cancer. Oncogene 39(17):3571–3587.

[30] He, Z., Khatib, A.M., Creemers, J.W.M., 2020. Loss of proprotein convertase furin in mammary gland impairs proIGF1R and proIR processing and suppresses tumorigenesis in triple negative breast cancer. Cancers 12(9).

[31] Ferris, H.A., Kahn, C.R., 2016. Unraveling the paradox of selective insulin resistance in the liver: the brain–liver connection. Diabetes 65(6):1481–1483.

[32] Inoue, H., 2016. Central insulin-mediated regulation of hepatic glucose production [Review]. Endocrine Journal 63(1):1–7.

[33] Könner, A.C., Janoschek, R., Plum, L., Jordan, S.D., Rother, E., Ma, X., et al., 2007. Insulin action in AgRP-expressing neurons is required for suppression of hepatic glucose production. Cell Metabolism 5(6):438–449.

[34] van Duijnhoven, H.L., Creemers, J.W., Kranenborg, M.G., Timmer, E.D., Groeneveld, A., van den Ouweland, A.M., et al., 1992. Development and characterization of a panel of monoclonal antibodies against the novel subtilisin-like proprotein processing enzyme furin. Hybridoma 11(1):71–86.

[35] Roebroek, A.J.M., Taylor, N.A., Louagie, E., Pauli, I., Smeijers, L., Snellinx, A., et al., 2004. Limited redundancy of the proprotein convertase furin in mouse liver. Journal of Biological Chemistry 279(51):53442–53450.

[36] Pritchard, L.E., Oliver, R.L., McLoughlin, J.D., Birtles, S., Lawrence, C.B., Turnbull, A.V., et al., 2003. Proopiomelanocortin-derived peptides in rat cerebrospinal fluid and hypothalamic extracts: evidence that secretion is regulated with respect to energy balance. Endocrinology 144(3):760–766.

[37] White, A., Gray, C., Ratcliffe, J.G., 1985. Characterisation of monoclonal antibodies to adrenocorticotrophin. Journal of Immunological Methods 79(2): 185–194.

[38] Crosby, S.R., Stewart, M.F., Ratcliffe, J.G., White, A., 1988. Direct measurement of the precursors of adrenocorticotropin in human plasma by two-site immunoradiometric assay. The Journal of Clinical Endocrinology and Metabolism 67(6):1272–1277.

[39] Rousseau, K., Kauser, S., Pritchard, L.E., Warhurst, A., Oliver, R.L., Slominski, A., et al., 2007. Proopiomelanocortin (POMC), the ACTH/melanocortin precursor, is secreted by human epidermal keratinocytes and melanocytes and stimulates melanogenesis. FASEB Journal 21(8):1844–1856.

[40] Wardlaw, S.L., 1986. Regulation of β-endorphin, corticotropin-like intermediate lobe peptide, and α-melanotropin stimulating hormone in the hypothalamus by testosterone. Endocrinology 119(1):19–24.

[41] Panigrahi, S.K., Meece, K., Wardlaw, S.L., 2019. Effects of naltrexone on energy balance and hypothalamic melanocortin peptides in male mice fed a high-fat diet. Journal of the Endocrine Society 3(3):590–601.

[42] Challis, B.G., Pritchard, L.E., Creemers, J.W.M., Delplanque, J., Keogh, J.M., Luan, J., et al., 2002. A missense mutation disrupting a dibasic prohormone processing site in pro-opiomelanocortin (POMC) increases susceptibility to early-onset obesity through a novel molecular mechanism. Human Molecular Genetics 11(17):1997–2004.

[43] Razolli, D.S., de Araújo, T.M., Sant Apos Ana, M.R., Kirwan, P., Cintra, D.E., Merkle, F.T., et al., 2020. Proopiomelanocortin processing in the

hypothalamus is directly regulated by saturated fat: implications for the development of obesity. Neuroendocrinology 110(1–2):92–104.

[44] Zheng, J., Zhang, L., Liu, J., Li, Y., Zhang, J., 2021. Long-term effects of maternal low-protein diet and post-weaning high-fat feeding on glucose metabolism and hypothalamic POMC promoter methylation in offspring mice. Frontiers in Nutrition 8:657848.

[45] Gali Ramamoorthy, T., Allen, T.J., Davies, A., Harno, E., Sefton, C., Murgatroyd, C., et al., 2018. Maternal overnutrition programs epigenetic changes in the regulatory regions of hypothalamic Pomc in the offspring of rats. International Journal of Obesity 42(8):1431–1444.

[46] Parton, L.E., Ye, C.P., Coppari, R., Enriori, P.J., Choi, B., Zhang, C.Y., et al., 2007. Glucose sensing by POMC neurons regulates glucose homeostasis and is impaired in obesity. Nature 449(7159):228–232.

[47] Jutras, I., Seidah, N.G., Reudelhuber, T.L., Brechler, V., 1997. Two activation states of the prohormone convertase PC1 in the secretory pathway. Journal of Biological Chemistry 272(24):15184–15188.

[48] Benjannet, S., Reudelhuber, T., Mercure, C., Rondeau, N., Chrétien, M., Seidah, N.G., 1992. Proprotein conversion is determined by a multiplicity of factors including convertase processing, substrate specificity, and intracellular environment. Cell type-specific processing of human prorenin by the convertase PC1. Journal of Biological Chemistry 267(16):11417–11423.

[49] Moehring, J.M., Moehring, T.J., 1983. Strains of CHO-K1 cells resistant to Pseudomonas exotoxin A and cross-resistant to diphtheria toxin and viruses. Infection and Immunity 41(3):998–1009.

[50] Zhou, A., Bloomquist, B.T., Mains, R.E., 1993. The prohormone convertases PC1 and PC2 mediate distinct endoproteolytic cleavages in a strict temporal order during proopiomelanocortin biosynthetic processing. Journal of Biological Chemistry 268(3):1763–1769.

[51] Alam, M.R., Steveson, T.C., Johnson, R.C., Bäck, N., Abraham, B., Mains, R.E., et al., 2001. Signaling mediated by the cytosolic domain of peptidylglycine alpha-amidating monooxygenase. Molecular Biology of the Cell 12(3):629–644.

[52] Dey, A., Lipkind, G.M., Rouillé, Y., Norrbom, C., Stein, J., Zhang, C., et al., 2005. Significance of prohormone convertase 2, PC2, mediated initial cleavage at the proglucagon interdomain site, lys70-arg71, to generate glucagon. Endocrinology 146(2):713–727.

[53] Jansen, E.J.R., Hafmans, T.G.M., Martens, G.J.M., 2010. V-ATPase-mediated granular acidification is regulated by the V-ATPase accessory subunit Ac45 in POMC-producing cells. Molecular Biology of the Cell 21(19):3330–3339.

[54] Stiernet, P., Guiot, Y., Gilon, P., Henquin, J.C., 2006. Glucose acutely decreases pH of secretory granules in mouse pancreatic islets. Mechanisms and influence on insulin secretion. Journal of Biological Chemistry 281(31): 22142–22151.

[55] Gowrisankaran, S., Milosevic, I., 2020. Regulation of synaptic vesicle acidification at the neuronal synapse. IUBMB Life 72(4):568–576.

[56] Nam, J.S., Ahn, C.W., Park, H.J., Kim, Y.S., 2020. Semaphorin 3 C is a novel adipokine representing exercise-induced improvements of metabolism in metabolically healthy obese young males. Science Report 10(1):10005.

[57] van der Klaauw, A.A., Croizier, S., Mendes de Oliveira, E., Stadler, L.K.J., Park, S., Kong, Y., et al., 2019. Human semaphorin 3 variants link melanocortin circuit development and energy balance. Cell 176(4), 729–742.e18.

[58] Seidah, N.G., Benjannet, S., Pareek, S., Chrétien, M., Murphy, R.A., 1996. Cellular processing of the neurotrophin precursors of NT3 and BDNF by the mammalian proprotein convertases. FEBS Letters 379(3):247–250.

[59] Marosi, K., Mattson, M.P., 2014. BDNF mediates adaptive brain and body responses to energetic challenges. Trends in Endocrinology and Metabolism 25(2):89–98.

